Asymptotic limits of some models for sound propagation in porous media and the assignment of the pore characteristic lengths

Kirill V. Horoshenkov[a)]
Department of Mechanical Engineering, University of Sheffield, Sheffield, S1 3JD, United Kingdom

Jean-Philippe Groby and Olivier Dazel
Laboratoire d'Acoustique de l'Université du Maine, Unité Mixte de Recherche 6613,
Centre National de la Recherche Scientifique, Université du Maine, F-72085 Le Mans Cedex 9, France

Modeling of sound propagation in porous media requires the knowledge of several intrinsic material parameters, some of which are difficult or impossible to measure directly, particularly in the case of a porous medium which is composed of pores with a wide range of scales and random interconnections. Four particular parameters which are rarely measured non-acoustically, but used extensively in a number of acoustical models, are the viscous and thermal characteristic lengths, thermal permeability, and Pride parameter. The main purpose of this work is to show how these parameters relate to the pore size distribution which is a routine characteristic measured non-acoustically. This is achieved through the analysis of the asymptotic behavior of four analytical models which have been developed previously to predict the dynamic density and/or compressibility of the equivalent fluid in a porous medium. In this work the models proposed by Johnson, Koplik, and Dashn [J. Fluid Mech. **176**, 379–402 (1987)], Champoux and Allard [J. Appl. Phys. **70**(4), 1975–1979 (1991)], Pride, Morgan, and Gangi [Phys. Rev. B **47**, 4964–4978 (1993)], and Horoshenkov, Attenborough, and Chandler-Wilde [J. Acoust. Soc. Am. **104**, 1198–1209 (1998)] are compared. The findings are then used to compare the behavior of the complex dynamic density and compressibility of the fluid in a material pore with uniform and variable cross-sections.
© 2016 Acoustical Society of America. [http://dx.doi.org/10.1121/1.4947540]

[FS]
Pages: 2463–2474

I. INTRODUCTION

The ability to accurately predict sound propagation in porous media is essential for many areas of science and engineering. Typical examples include non-invasive inspection of porous bones, outdoor sound propagation in presence of porous ground, underwater sound propagation in the presence of porous sediments, and noise control. A majority of models which are used for these purposes are equivalent fluid models in which the fluid trapped in the material pores is typically presented as a homogeneous, equivalent fluid with complex, frequency dependent acoustic characteristic impedance, $z(\omega)$, and complex wavenumber, $k(\omega)$. Here $\omega = 2\pi f$ is the angular frequency, where f is the frequency in Hz. In practical calculations these are usually the properties of bulk medium, rather than to the fluid properties in a single pore. The value of the characteristic impedance and the boundary conditions surrounding the porous layer determine the ability of sound waves to penetrate this layer. The value of the complex wavenumber relates to the speed of the sound wave in the porous space and the rate at which it attenuates.

The models used to predict the acoustic impedance and wavenumber require the accurate knowledge of several intrinsic material parameters some of which are difficult to measure non-acoustically. A most common class of these models is based on the works by Johnson *et al.*[1] and Champoux and Allard.[2] Johnson *et al.* introduced the concept of the viscous characteristic length which is the ratio [see Eq. (2.17) in Ref. 1]

$$\Lambda = 2\frac{\int |\mathbf{u}(\mathbf{r})|^2 dV}{\int |\mathbf{u}(\mathbf{r_w})|^2 dA},$$ (1)

where $\mathbf{u}(\mathbf{r})$ is the seepage velocity vector of the fluid in the material pores which is excited by the incident sound wave. The integration in the denominator of Eq. (1) is carried out over the pore-frame interface of the pore area, A, whereas the integration in the numerator in Eq. (1) is carried out with respect to the pore volume, V. According to Johnson *et al.*, "Λ is the volume-to-surface ratio of the pore-solid interface in which each area or volume element is weighted according to the local value of the field $\mathbf{u}(\mathbf{r})$."[1] The main use of the viscous characteristic length is to define the characteristic pore scale so that the complex, frequency dependent dynamic tortuosity [Eq. (3.4a) in Ref. 1]

$$\tilde{\alpha}(\omega) = \alpha_{\infty}\left[1 + \frac{\sigma\phi}{i\alpha_{\infty}\rho_0\omega}\left(1 + \frac{4i\alpha_{\infty}^2\eta\rho_0\omega}{\sigma^2\Lambda^2\phi^2}\right)^{1/2}\right]$$ (2)

and the dynamic density [Eq. (3) in Ref. 2]

[a)]Electronic mail: k.horoshenkov@sheffield.ac.uk

$$\tilde{\rho}(\omega) = \tilde{\alpha}(\omega)\rho_0/\phi \qquad (3)$$

of the fluid which fills the material pores can be predicted. In the above equations ρ_0 is the equilibrium fluid density, α_∞ is the geometric tortuosity, σ is the static air flow resistivity, η is the dynamic viscosity of the fluid, ϕ is the material porosity, and $i = \sqrt{-1}$. According to Johnson et al., the dynamic density is related to the dynamic permeability as

$$\tilde{\kappa}(\omega) = \frac{i\eta\phi}{\tilde{\alpha}(\omega)\omega} \qquad (4)$$

[Eq. (2.1c) in Ref. 1]. In many cases, the Johnson et al. model is used with the low frequency viscous permeability, $\kappa_0 = \lim_{\omega \to 0} \kappa(\omega)$, so that the flow resistivity, σ, is replaced with $\kappa_0 = \eta/\sigma$ to avoid the influence of the properties of the saturating fluid. It is worth noting that the expression of the dynamic density we present in this paper [Eq. (3)] is given for the bulk medium; therefore, it is normalized by the medium porosity ϕ. In this sense, Eq. (3.4a) for the dynamic tortuosity in Ref. 1 and Eq. (3) for the dynamic density in Ref. 2 are given for a sound propagation in a single pore and these need normalizing by ϕ if used to describe the bulk medium. The tilde over a symbol in the above equations and in the following text suggest that the frequency-dependent quantity is for the fluid in a pore which cross-section varies along the pore length.

There are a number of reliable non-acoustic laboratory techniques to measure the porosity, tortuosity, and flow resistivity (or viscous permeability) which are well detailed in Chap. 5 in Ref. 3. However, measuring the viscous characteristic length seems rather problematic. Traditionally, the value of Λ has either been adjusted to make the model fit (e.g., see Sec. IV in Ref. 2) or estimated from the high-frequency behavior of the dynamic density (e.g., Refs. 5 and 6) or from the impedance tube data (e.g., Ref. 7).

The model proposed by Johnson et al.[1] works well for a porous medium which can be approximated with a network of non-intersecting tubes with a uniform cross-section. For the materials with non-uniform pores, the knowledge of Λ is not sufficient to account for the thermal dissipation effects and to satisfy the actual asymptotic behavior of the frequency-dependent sound speed in this type of porous media in the low- and high-frequency limits. The viscous losses are larger in the narrowest parts of the pore and these parts are described with the characteristic dimension Λ. The thermal losses are larger in the wider parts of the pore which need to be characterized with the thermal characteristic length. Champoux and Allard[2] suggested that these effects should be properly accounted for through the dynamic bulk modulus, which is given by

$$\tilde{K}(\omega) = \frac{\gamma P_0}{\phi} \left[\gamma - \frac{\gamma - 1}{1 - \dfrac{i\sigma'\phi}{\rho_0 \alpha_\infty N_{Pr}\omega} \left(1 + \dfrac{4i\alpha_\infty^2 \eta \rho_0 N_{Pr}\omega}{\left(\sigma'\Lambda'\phi\right)^2} \right)^{1/2}} \right]^{-1}. \qquad (5)$$

Here σ' is the thermal flow resistivity, Λ' is the thermal characteristic length describing the pore scale where the thermal dissipation effects are particularly pronounced, and N_{Pr} is the Prandtl number. More commonly, the thermal flow resistivity, σ', is replaced with its thermal permeability counterpart, i.e., $\kappa_0' = \eta/\sigma'$. In the case of a material with non-uniform pores Λ' can be significantly different from Λ and $\Lambda' > \Lambda$. It is defined as twice the ratio of the fluid volume in the pores to the pore surface area in this volume, i.e.,

$$\Lambda' = 2\frac{\int dV}{\int dA}. \qquad (6)$$

Because $\sigma \sim \Lambda^{-2}$ and $\sigma' \sim \Lambda'^{-2}$, it is usual that $\sigma > \sigma'$.[2] The characteristic impedance and wavenumber of this type of porous media can be then predicted using the density and compressibility information

$$\tilde{z}(\omega) = \sqrt{\tilde{\rho}(\omega)/\tilde{C}(\omega)} \text{ and } \tilde{k}(\omega) = \omega\sqrt{\tilde{\rho}(\omega)\tilde{C}(\omega)}, \qquad (7)$$

where $\tilde{C}(\omega) = 1/\tilde{K}(\omega)$ is the complex compressibility of fluid in the material pores and $\tilde{c}(\omega) = \sqrt{\tilde{\rho}(\omega)\tilde{C}(\omega)}$ is the sound speed. It has been shown that this model works well for a wide range of porous media with arbitrary pore geometry and pore size distribution, e.g., in the case of fibrous materials (Sec. IV in Ref. 4), granular media,[9] and foams (Sec. V in Ref. 10). The combination of Eqs. (2), (3), and (5) is usually called the Johnson-Champoux-Allard model or JCA model.

The question is how to determine the values of the thermal characteristic length, Λ', and thermal permeability, κ_0', needed for the JCA model. These parameters are rarely measured non-acoustically.[5,6] There are efficient acoustical methods to measure these parameters (e.g., Refs. 7 and 8). The purpose of this paper is to illustrate how the parameters Λ, Λ', and κ_0' can be related to the pore size distribution in a porous medium, which is a routinely measurable characteristics using a number of affordable laboratory methods which include the water saturation, gas adsorption, and optical analysis techniques. In a particular case, when the pore size distribution is log-normal, this paper shows that the parameters used in the models of Johnson et al.,[1] Champoux and

2464   J. Acoust. Soc. Am. **139** (5), May 2016

Horoshenkov et al.

Allard,[2] and Pride *et al.*[14] (see Sec. II B) can be expressed as a function of the mean pore size and standard deviation. The paper is organized as follows. Section II compares the asymptotic behavior of the dynamic density for the case when the pore shape and size are assumed to be uniform along the pore length, but the medium can be composed of pores of various cross-sectional area. Section III derives the exact expressions for the dynamic density and complex compressibility for the porous medium for the case, when the pore shape is assumed to be circular cylindrical shape, but pore size is no longer uniform along the pore length. We present the fundamental relations between the intrinsic material parameters used in the different models. We also derive the new Padé approximations for the dynamic density and complex compressibility of fluid filling the non-uniform pores. Section IV compares the behavior of several models for the acoustical properties of porous medium against the new model. The conclusions are drawn in Sec. V.

II. SOUND PROPAGATION IN UNIFORM CYLINDRICAL PORES

A. Theoretical background

Let us first consider the case when a sound wave propagates in a medium which can be described as a stack of uniform cylindrical pores which cross-sectional area is randomly distributed, but does not change in the axial direction as illustrated in Fig. 1. For this type of porous media, it was shown that the dynamic density of the effective fluid in a single pore in a material averaged over all possible pore sizes can be given by the following expression:[11]

$$\rho_x(\omega) = \rho_0 \frac{1}{1 - I(\omega)},$$

(8)

where

$$I(\omega) = 1 - \frac{i\omega\rho_0}{\eta} \int_0^\infty s^2 e(s)\psi(\omega, s)ds.$$

(9)

Here and below, the subscript x suggests that we refer to a quantity which describes sound propagation in a single pore. The function $\psi(\omega, s)$ in integral (9) is the solution of the
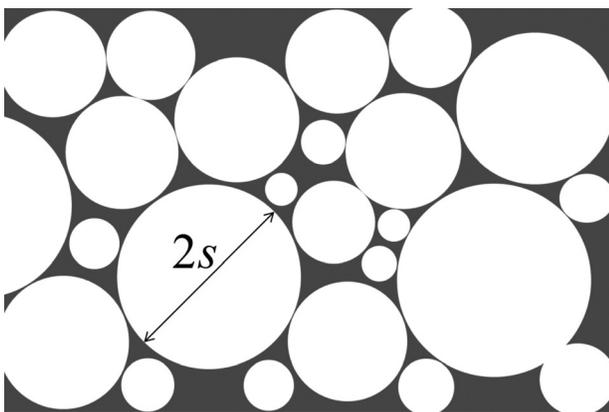
FIG. 1. A porous medium consisting of uniform pores with random cross-section.

Helmholtz equation for the acoustic velocity field in the material pore of size s. It depends on the adopted pore geometry and frequency of sound and its physical meaning is discussed in Sec. I in Ref. 11. The term $e(s)$ in integral (9) is the probability density function for the distribution of the pore radius s. For a particular case when the pore geometry is circular,

$$\psi(z) = \left(\frac{2I_1(z)}{zI_0(z)} - 1\right)z^{-2},$$

(10)

where $z = s\sqrt{-i\omega\rho_0/\eta}$ and $I_0(z)$ and $I_1(z)$ are the modified Bessel functions of order zero and one, respectively.[12]

If the porous material is composed of pores which radii s obey a log-normal distribution, i.e., $e(\varphi) = (1/\sigma_s\sqrt{2\pi})e^{-(\varphi-\bar{\varphi})^2/2\sigma_s^2}$, $\varphi = -\log_2 s$, $\bar{\varphi} = -\log_2\bar{s}$, then the expression for $I(\omega)$ in Eq. (8) can be given by the following integral:

$$I(\omega) = \frac{1}{\sqrt{2\pi}} \int_{-\infty}^{+\infty} \chi(\bar{z} \, 2^{-\sigma_s t})e^{-t^2/2}dt,$$

(11)

where $\bar{z} = \bar{s}\sqrt{-i\omega\rho/\eta}$ and $\bar{s}$ is the median pore size. This type of pore size distribution is highly common for granular porous media and foams (e.g., Ref. 13). We note that the standard deviation σ_s is a measure of the log-normal distribution and it is given in terms of the φ units, where $\bar{\varphi} = -\log_2\bar{s}$ is the average pore size taken on the log-normal scale. The function χ in integral (11) depends only on the assumed pore shape and frequency. In the case of circular cylindrical pores of radius s we chose in this work, this function is

$$\chi(z) = \frac{2I_1(z)}{zI_0(z)}.$$

(12)

Alternative forms of $\chi(z)$ for other pore geometries are available and discussed in Sec. II in Ref. 11. We note that the choice of pore shape does not make a significant difference in the frequency range when the acoustic wavelength is much larger than the characteristic pore size. In this case, the pore size distribution has the dominant effect.

Expression (8) can be used to define the complex compressibility of the fluid in a single pore which is given by

$$C_x(\omega) = \frac{1}{\gamma P_0}\left(\gamma - \frac{\rho_0(\gamma - 1)}{\rho_x(N_{pr}\omega)}\right).$$

(13)

In order to represent the acoustical properties of a bulk medium with tortuous pores occupying a representative proportion of the material volume, we need to account for the pore tortuosity and material porosity. In this case we require that the mean velocity through the pores in the bulk medium, i.e., the total volume flux divided by the cross-sectional area of the sample is $\langle u \rangle = \phi\langle u_x \rangle/\sqrt{\alpha_\infty}$, where $\langle u_x \rangle$ is the mean velocity in a single pore in a porous medium with some statistically distributed pore size as defined with $e(\varphi)$. In order to satisfy the equation of motion [Eq. (9) in Ref. 11] and the equation of thermodynamic equilibrium [Eq. (19) in Ref. 11] in the case of the bulk medium, we need to replace $\rho_x(\omega)$ by a bulk medium dynamic complex density,

J. Acoust. Soc. Am. **139** (5), May 2016

Horoshenkov *et al.*   2465

$$\rho(\omega) = \frac{\alpha_\infty}{\phi}\rho_x(\omega), \qquad (14)$$

and complex compressibility with its bulk characteristic,

$$C(\omega) = \phi C_x(\omega). \qquad (15)$$

Here we also need to introduce the bulk flow resistivity, $\sigma = \alpha_\infty \sigma_x/\phi$, which replaces the flow resistivity of a single pore, σ_x. The pore size distribution model suggests that the flow resistivity of a single pore in a material with statistical pore size distribution $e(s)$ is given by the following expression (see Sec. III in Ref. [11]):

$$\sigma_x = \frac{-\eta}{\bar{\psi}_0 \langle s^2 \rangle} = \frac{-\eta}{\bar{\psi}_0 \bar{s}^2 e^{2\zeta}}, \qquad (16)$$

where $\langle s^2 \rangle = \int_0^\infty s^2 e(s)ds$ is the mean pore size, $\bar{s}$ is the median pore size and the coefficient $\bar{\psi}_0 = -1/8$ for the adopted circular, cylindrical pore geometry (see Table I in Ref. [11]) and $\zeta = (\sigma_s \log 2)^2$.

B. Behavior of the uniform pore models at asymptotic limits

The low- and high-frequency behavior of the dynamic density of the equivalent fluid in a single pore for a material with a log-normal pore size distribution can be expressed with the following asymptotic limits (see Sec. III in Ref. [11]):

$$\frac{\rho_x(\omega)}{\rho_0} = \frac{1}{\varepsilon^2} + 1 + \theta_1 + O(\varepsilon^2), \ \varepsilon \to 0 \qquad (17)$$

and

$$\frac{\rho_x(\omega)}{\rho_0} = 1 + \frac{\theta_2}{\varepsilon} + O(\varepsilon^{-2}), \ \varepsilon \to \infty, \qquad (18)$$

where $\varepsilon = \sqrt{-i\omega\rho_0/\sigma_x}$. The coefficients θ_1 and θ_2 are real positive coefficients whose values depend only on the assumed pore shape. In the case of the circular pore shape, these coefficients are $\theta_1 = 4/3 e^{4\zeta} - 1$ and $\theta_2 = 1/\sqrt{2} e^{3/2\zeta}$ (see Table I in Ref. [11]). In light of the above, we can rewrite expressions (17) and (18) to obtain the following two asymptotic limits:

$$\frac{\rho_x(\omega)}{\rho_0} = \frac{\sigma_x}{-i\omega\rho_0} + 4/3 e^{4(\sigma_s \ln 2)^2} + O(\omega), \ \omega \to 0 \qquad (19)$$

and

$$\frac{\rho_x(\omega)}{\rho_0} = 1 + \frac{2 e^{1/2(\sigma_s \ln 2)^2}}{\bar{s}}\sqrt{\frac{\eta}{-i\omega\rho_0}} + O(\omega^{-1}), \ \omega \to \infty. \qquad (20)$$

In Ref. [11] these asymptotic limits were used to derive the Padé approximation for the Biot's viscosity correction function. This approximation depends on the complex variable ε and it helps to avoid a requirement for numerical integration or evaluation of special functions in integral (11) when the complex dynamic density and complex

compressibility need to be calculated [expressions (8) and (13)]. It is of interest to compare the coefficients at these two limits with the coefficients in the limits of the model by Johnson et al.[1] and Pride et al.[14]

According to the model by Johnson et al.[1] the low-frequency asymptotic limits for the behavior of the dynamic density in a material composed of straight cylindrical pores of circular shape is

$$\frac{\rho_x(\omega)}{\rho_0} = \frac{\sigma_x}{-i\omega\rho_0} + \left(1 + \frac{2\eta}{\sigma_x\Lambda^2}\right) + O(\omega), \ \omega \to 0. \qquad (21)$$

In the case of a circular cylindrical pore $\sigma_x = 8\eta/\Lambda^2$, so that we have

$$\frac{\rho_x(\omega)}{\rho_0} = \frac{\sigma_x}{-i\omega\rho_0} + \frac{5}{4} + O(\omega), \ \omega \to 0. \qquad (22)$$

An alternative formulation for the low-frequency asymptotic behavior of the dynamic density can be derived using the approach proposed by Pride et al.,[14]

$$\frac{\rho_x(\omega)}{\rho_0} = 1 + \beta + \frac{\sigma_x}{-i\omega\rho_0}, \ \omega \to 0, \qquad (23)$$

where β is a coefficient introduced by Pride et al. It is related to the enhancement in the effective fluid inertia at lower frequencies caused by the cross-sectional changes in the pore size and viscous friction on the smallest apertures of the pore.[14] The asymptotic behavior of the dynamic density at the higher frequency end of the spectrum given by Johnson et al. is

$$\frac{\rho_x(\omega)}{\rho_0} = 1 + \frac{2}{\Lambda}\sqrt{\frac{\eta}{-i\omega\rho_0}} + O(\omega^{-1}), \ \omega \to \infty. \qquad (24)$$

We note that the expression for the dynamic density in the model proposed in Ref. [1] differs from that proposed in Ref. [14] by the asymptotic behavior of the low-frequency limit.

The comparison of equations (20) and (21) suggests that it is impossible to match the asymptotic behavior of the real part of the dynamic density derived for $\omega \to 0$ in the case of the pore size distribution approach[11] and the model of Johnson et al.[1] It can be matched exactly to that of the model of Pride et al.[14] if the parameter β in the Pride et al. model is set to $\beta = 4/3 e^{4(\sigma_s \ln 2)^2} - 1$. The asymptotic behavior of the imaginary part of the dynamic density derived for $\omega \to 0$ is exactly the same for all these two models. A comparison of expressions (20) and (24) suggests that the behavior of the dynamic density at the $\omega \to \infty$ limit can be matched exactly provided that $\Lambda = \bar{s} e^{-1/2(\sigma_s \ln 2)^2}$.

III. SOUND PROPAGATION IN NON-UNIFORM CYLINDRICAL PORES

A. Theoretical background

Let us now consider sound propagation in a cylindrical pore which circular cross-section varies with depth as shown in Fig. 2. We split this pore in N sections and assume that within each of these sections the flow velocity ν_n and pore

Horoshenkov *et al.*

cross-sectional area A_n are constant. We denote q to be the volume velocity in the oscillatory flow which is set through this pore because of the acoustic pressure p is applied to its throat. We follow the original work by Champoux and Stinson[15] and assume that the length of the pore Δx is long enough to include a representative number of pore scale variations but much shorter than the acoustic wavelength. We assume that the pore cross-section is circular so that the dynamic density and complex compressibility of the fluid in each of the pore sections illustrated in Fig. 2 can be expressed as [Eqs. (9) and (12) in Ref. 16]

$$\rho_x(\omega) = \rho_0/(1 - 2T(z)/z) \tag{25}$$

and

$$C_x(\omega) = \frac{1}{\gamma P_0} \left(\gamma - \frac{\rho_0(\gamma - 1)}{\rho_x(\sqrt{N_{Pr}}z)} \right), \tag{26}$$

respectively. In the above expressions $T(z) = J_1(z)/J_0(z)$ is the ratio of the Bessel functions and $z = s\sqrt{-i\omega\rho_0/\eta}$ as before.

Here we are interested in the behavior of functions $\rho_x(\omega)$ and $C_x(\omega)$ in the low ($z \to 0$) and high ($z \to \infty$) frequency limits. For this purpose, we make use of the following asymptotic behavior of the function $2T(z)/z$:

$$2T(z)/z = 1 - z^2/8 + z^4/48 + O(z^6), \ z \to 0, \tag{27}$$

and

$$2T(z)/z = 2/z - 1/z^2 + O(z^{-3}), \ z \to \infty. \tag{28}$$

The above yields

$$\begin{aligned} &\rho_x(\omega) = \rho_0(4/3 + 8/z^2) + O(z^4), \\ &C_x(\omega) = \frac{1}{\gamma P_0} \left(\gamma + (\gamma - 1)N_{Pr}z^2/8 \right) + O(z^4), \ z \to 0 \end{aligned} \tag{29}$$

and
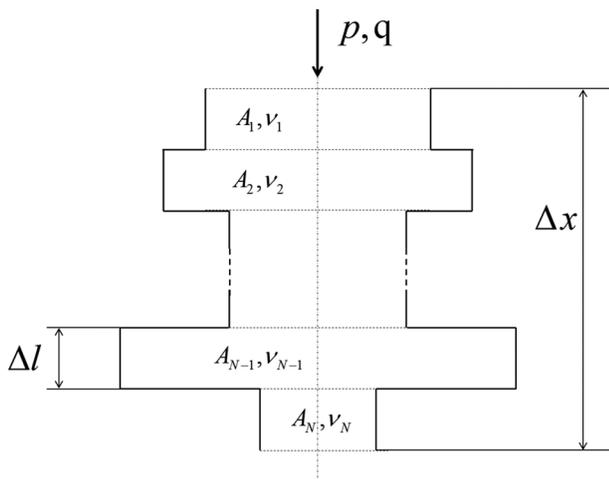
FIG. 2. Sound propagation in a non-uniform pore.

$$\begin{aligned} &\rho_x(\omega) = \rho_0(1 + 2/z) + O(z^{-2}), \\ &C_x(\omega) = \frac{1}{\gamma P_0} \left(1 - 2(\gamma - 1)/(z\sqrt{N_{Pr}}) \right) \\ &\qquad\qquad + O(z^{-2}), \ z \to \infty. \end{aligned} \tag{30}$$

Let us now consider that the acoustic pressure p is applied across the pore length Δx as depicted in Fig. 2. The equation of motion for the fluid in this pore is

$$-\frac{\partial p}{\partial x} = i\omega\tilde{\rho}_x(\omega)\nu, \tag{31}$$

where $\tilde{\rho}_x(\omega)$ is the frequency-dependent dynamic density of the fluid in the non-uniform pore, and ν is the mean flow velocity in the pore. The problem here is to determine the density function $\tilde{\rho}_x(\omega)$ for the mean flow velocity in the pore, which is

$$\nu = 1/N \sum_n \nu_n = q/N \sum_n 1/A_n. \tag{32}$$

The pressure change over the part of this pore with the cross-section A_n is

$$-\Delta p_n = i\omega q \rho_n(\omega)/A_n dl, \tag{33}$$

where $\rho_n(\omega)$ is the dynamic density of the fluid in the part of the pore with the area $A_n = \pi s_n^2$, which can be expressed with Eq. (25) in which the pore radius in the parameter z is set to $s = s_n$. The total pressure change over the whole pore length Δx is

$$\Delta p = \sum_n \Delta p_n, \tag{34}$$

i.e.,

$$-\Delta p = i\omega q \sum_n \rho_n(\omega)/A_n dl. \tag{35}$$

The pressure gradient over the total pore length Δx is

$$-\frac{\Delta p}{\Delta x} = i\omega q \sum_n \rho_n(\omega)/A_n dl/\Delta x. \tag{36}$$

Because $q = \nu/(1/N \sum_n 1/A_n)$ and $dl/\Delta x = 1/N$, we obtain

$$-\frac{\Delta p}{\Delta x} = i\omega \frac{\displaystyle\sum_n \rho_n(\omega)/A_n}{\displaystyle\sum_n 1/A_n} \nu, \tag{37}$$

where

$$\tilde{\rho}_x(\omega) = \frac{\displaystyle\sum_n \rho_n(\omega)/A_n}{\displaystyle\sum_n 1/A_n} \tag{38}$$

is the expression for the dynamic density in the nonuniform pore. The $N \to \infty$ and $dl \to 0$ limit of the above expression is ($s_n \to s$)

$$\tilde{\rho}_x(\omega) = \frac{\int_0^\infty \rho_x(\omega,s)e(s)/s^2 ds}{\int_0^\infty e(s)/s^2 ds} = \frac{I_\rho}{I_{1/A}}, \qquad (39)$$

where $e(s)$ is the probability density function for the distribution of the pore size s along the length of the pore.

Similarly, we can derive the expression for the complex compressibility function $\tilde{C}_x(\omega)$ making use of the continuity equation for the oscillatory flow of fluid in the non-uniform pore, i.e.,

$$-\frac{\partial \nu}{\partial x} = i\omega \tilde{C}_x(\omega)p. \qquad (40)$$

Under the influence of the acoustic pressure p applied to the pore neck the change in the flow velocity in the part of the pore with cross-section A_n is

$$-\Delta \nu_n = i\omega C_n(\omega)pdl, \qquad (41)$$

where $C_n(\omega)$ is the compressibility of the fluid in this part of the pore which can be predicted using Eq. (26) for $s = s_n$. Assuming that the acoustic pressure is constant over Δx the total change in the volume velocity over the length Δx is the sum

$$-\frac{\Delta q}{\Delta x} = -\sum_n \Delta \nu_n A_n = i\omega \sum_n C_n(\omega)A_n pdl/\Delta x. \qquad (42)$$

Because of $dl/\Delta x = 1/N$ and $\Delta q = \Delta \nu/N \sum_n A_n$, where $\Delta \nu$ is the average velocity variation across the length Δx, the above equation becomes

$$-\frac{\Delta \nu}{\Delta x} = i\omega \frac{\sum_n C_n(\omega)A_n}{\sum_n A_n}p, \qquad (43)$$

where

$$\tilde{C}_x(\omega) = \frac{\sum_n C_n(\omega)A_n}{\sum_n A_n} \qquad (44)$$

is the complex compressibility of the fluid in the non-uniform pore. The $N \to \infty$ and $dl \to 0$ limit of the above expression is

$$\tilde{C}_x(\omega) = \frac{\int_0^\infty C_x(\omega,s)e(s)s^2 ds}{\int_0^\infty e(s)s^2 ds} = \frac{I_C}{I_A}. \qquad (45)$$

B. The asymptotic limits for the dynamic density and compressibility for the fluid in a non-uniform pore

In this section we will study the asymptotic limits for the dynamics density [Eq. (39)] and complex compressibility

[Eq. (45)] which we derived in Sec. III A. As before, we assume that the pore radius is distributed log-normally, i.e., $e(s) = f(\varphi)(d\varphi/ds)$, where $f(\varphi) = (1/\sigma_s\sqrt{2\pi})e^{-(\varphi-\bar{\varphi})^2/2\sigma_s^2}$ and $\varphi = -\log_2 s$. The problem now is to estimate the low-frequency limit ($\omega \to 0$) of Eqs. (39) and (45),

$$\tilde{\rho}_x(\omega) = \frac{I_\rho}{I_{1/A}} \qquad (46)$$

and

$$\tilde{C}_x(\omega) = \frac{I_C}{I_A}, \qquad (47)$$

where the integrals in the denominator are expressed in terms of the parameters of the log-normal distribution σ_s, $\bar{\varphi}$, and φ,

$$I_\rho = \int_{-\infty}^{+\infty} \rho_x(\omega,\varphi)2^{2\varphi}e^{-(\varphi-\bar{\varphi})^2/2\sigma_s^2}d\varphi, \qquad (48)$$

$$I_{C,\omega} = \int_{-\infty}^{+\infty} C_x(\omega,\varphi)2^{-2\varphi}e^{-(\varphi-\bar{\varphi})^2/2\sigma_s^2}d\varphi, \qquad (49)$$

$$I_{1/A} = \int_{-\infty}^{+\infty} 2^{2\varphi}e^{-(\varphi-\bar{\varphi})^2/2\sigma_s^2}d\varphi = \sqrt{2\pi}\sigma_s 2^{2\bar{\varphi}}e^{2\sigma_s^2 \log^2 2}, \qquad (50)$$

and

$$I_A = \int_{-\infty}^{+\infty} 2^{-2\varphi}e^{-(\varphi-\bar{\varphi})^2/2\sigma_s^2}d\varphi = \sqrt{2\pi}\sigma_s 2^{-2\bar{\varphi}}e^{2\sigma_s^2 \log^2 2}. \qquad (51)$$

The Appendix presents the detailed procedure which we used to derive the low- and high-frequency limits of the integrals I_ρ and I_C. The Appendix also shows how the integrals $I_{1/A}$ and I_A can be reduced to some simple analytical expressions.

The results presented in the appendix suggest that the asymptotic limits for the dynamic density and complex compressibility of fluid in a non-uniform pore can be expressed as

$$\tilde{\rho}_x(\omega) = \rho_0\left(4/3 - \frac{8\eta e^{6\sigma_s^2 \log^2 2}}{i\omega\rho_0 \bar{s}^2}\right) + O(\omega^2), \ \omega \to 0, \qquad (52)$$

$$\tilde{C}_x(\omega) = \frac{1}{\gamma P_0}\left(\gamma - (\gamma-1)\frac{i\omega\rho_0 N_{Pr}\bar{s}^2 e^{6\sigma_s^2 \log^2 2}}{8\eta}\right) + O(\omega^2), \ \omega \to 0, \qquad (53)$$

$$\tilde{\rho}_x(\omega) = \rho_0\left(1 + \frac{2e^{5/2\sigma_s^2 \log^2 2}}{\bar{s}}\sqrt{\frac{\eta}{-i\omega\rho_0}}\right) + O(\omega^{-1}), \ \omega \to \infty, \qquad (54)$$

and

$$\tilde{C}_x(\omega) = \frac{1}{\gamma P_0} \left(1 - \frac{2e^{-3/2\sigma_s^2 \log^2 2}}{\bar{s}} \sqrt{\frac{\eta}{-i\omega\rho_0 N_{Pr}}} \right) + O(\omega^{-1}), \ \omega \to \infty. \tag{55}$$

These limits enable us to derive the relations between the characteristic lengths and permeabilities used in the JCA model and pore size distribution parameters which we used in the Champoux-Stinson representation of the non-uniform pore. The behavior of the dynamic density in the low frequency limit [Eq. (52)] yields the following values of the flow resistivity and viscous permeability:

$$\sigma_x = \frac{8\eta}{\bar{s}^2} e^{6(\sigma_s \log 2)^2} \tag{56}$$

and

$$\kappa_0 = \frac{\bar{s}^2}{8} e^{-6(\sigma_s \log 2)^2}, \tag{57}$$

respectively. The application of Eq. (53) and Eq. (5.6) in Ref. 3 yields the following values of the thermal resistivity and permeability:

$$\sigma'_x = \frac{8\eta}{\bar{s}^2} e^{-6(\sigma_s \log 2)^2} \tag{58}$$

and

$$\kappa'_0 = \frac{\bar{s}^2}{8} e^{6(\sigma_s \log 2)^2}. \tag{59}$$

The above suggests that the ratio of the thermal to viscous permeabilities is $\kappa'_0/\kappa_0 = e^{12(\sigma_s \log 2)^2}$. For a typical value of $\sigma_s = 0.3$, this ratio is 1.680. The values of the viscous and thermal permeabilities are equal in the case of a uniform pore, i.e., when $\sigma_s = 0$. The leading term of 4/3 in Eq. (52) is consistent with the parameter $\beta = 1/3$ in Eq. (23) proposed by Pride *et al.*[14] to improve the low frequency behavior of the model by Johnson *et al.* [see Eqs. (2) and (3)]. It is related to the enhancement in the effective fluid inertia at lower frequencies caused by the cross-sectional changes in the pore size and viscous friction on the smallest apertures of the pore. In some more recent publications this parameter has been modified and assigned with notations other than β which was originally used by Pride *et al.* [e.g., parameter P in Eq. (25) in Ref. 17, parameter b in Eq. (5.32) in Ref. 3]. It is of interest to note that in the case of a porous medium with cylindrical pores which radius is log-normally distributed (see Sec. II B), the Pride parameter is equivalent to $\beta = 4/3 e^{4(\sigma_s \ln 2)^2} - 1$.

The behavior of the dynamics density and compressibility in the high frequency limit [Eqs. (24), (54), (55), and Eq. (28) in Ref. 4] yields the following values of the viscous and thermal characteristic lengths:

$$\Lambda = \bar{s} e^{-5/2(\sigma_s \log 2)^2} \tag{60}$$

and

$$\Lambda' = \bar{s} e^{3/2(\sigma_s \log 2)^2}, \tag{61}$$

respectively. It is clear that the ratio of these two lengths is $\Lambda'/\Lambda = e^{4(\sigma_s \log 2)^2}$. For the value of the standard deviation chosen in the previous example ($\sigma_s = 0.3$) this ratio is 1.189. The characteristic lengths become identical in the uniform pore case. We note that there is an error in Eq. (28) in Ref. 4. Its denominator should refer to Λ' instead of Λ.

C. Padé approximations

Equations for the asymptotic limits (52)–(55) provide a good basis to understand the relations between various intrinsic material parameters used in a range of models for the acoustical properties of porous media. However, these are inconvenient to calculate the acoustical properties of the fluid in a non-uniform pore. In the work by Horoshenkov *et al.*[11] it was suggested to adopt the Padé approximation to link the two limits together. It is possible to modify the Padé approximation used in Ref. 11 to account for the results presented in Sec. III B.

Following the work by Horoshenkov *et al.*[11] we express Eqs. (52) and (54) for the dynamic density in a form similar to Eqs. (17) and (18),

$$\tilde{\rho}_x(\epsilon)/\rho_0 = 1 + \theta_{\rho,1} + \epsilon_\rho^{-2} + O(\epsilon_\rho^4), \ \epsilon \to 0 \tag{62}$$

and

$$\tilde{\rho}_x(\epsilon)/\rho_0 = 1 + \theta_{\rho,2}\epsilon_\rho + O(\epsilon_\rho^{-2}), \ \epsilon_\rho \to \infty, \tag{63}$$

respectively. In the above equations we denote $\epsilon_\rho = \sqrt{-i\omega\rho_0/\sigma_x}$. The coefficient $\theta_{\rho,1} = 1/3$ is essentially the parameter of Pride *et al.*[14] which depends on the pore cross-sectional shape only. It is also equivalent to the coefficient θ_1 used in the Padé approximation in Ref. 11 [see Eq. (53) in Ref. 11]. The coefficient $\theta_{\rho,2} = e^{-1/2(\sigma_s \log 2)^2}/\sqrt{2}$ is equivalent to the Padé coefficient θ_2 [see Eq. (56) in Ref. 11] which depends both on the pore cross-sectional shape and on the width of the pore size distribution.

Following Ref. 11 (see pages 1205 and 1206) we suggest approximating the dynamic density with the following expression:

$$\tilde{\rho}_x(\epsilon_\rho) \simeq 1 + \epsilon_\rho^{-2}\tilde{F}_\rho(\epsilon_\rho), \tag{64}$$

where

$$\tilde{F}_\rho(\epsilon_\rho) = \frac{1 + \theta_{\rho,3}\epsilon_\rho + \theta_{\rho,1}\epsilon_\rho}{1 + \theta_{\rho,3}\epsilon_\rho} \tag{65}$$

is the Padé approximant and $\theta_{\rho,3} = \theta_{\rho,1}/\theta_{\rho,2}$.

A very similar procedure can be adopted to derive the Padé approximation for the complex compressibility. First, we make use of Eq. (26) to express Eqs. (53) and (55) in the following form:

$$\gamma P_0 \tilde{C}_x(\epsilon_c) = \gamma + (\gamma - 1)\epsilon_c^2 + O(\epsilon_c^4), \ \epsilon_c \to 0 \tag{66}$$

and

J. Acoust. Soc. Am. **139** (5), May 2016

Horoshenkov *et al.* 2469

$$\gamma P_0 \tilde{C}_x(\epsilon_c) = 1 - \theta_{c,2}\epsilon_c^{-1} + O(\epsilon_c^{-2}), \ \epsilon_c \to \infty, \qquad (67)$$

where $\epsilon_c = \sqrt{(-i\omega\rho_0 N_{Pr}/\sigma'_x)}$ and $\theta_{c,2} = e^{3/2(\sigma_s \log 2)^2}/\sqrt{2}$. In this case, the complex compressibility can be approximated with

$$\tilde{C}_x(\epsilon_c) = \frac{1}{\gamma P_0}\left(\gamma - \frac{\gamma - 1}{1 + \epsilon_c^{-2}\tilde{F}_c(\epsilon_c)}\right), \qquad (68)$$

where

$$\tilde{F}_c(\epsilon_c) = \frac{1 + \theta_{c,3}\epsilon_c + \theta_{c,1}\epsilon_c}{1 + \theta_{c,3}\epsilon_c}. \qquad (69)$$

We note that in the above approximation $\theta_{c,1} = \theta_{\rho,1} = 1/3$ and that $\theta_{c,3} = \theta_{c,1}/\theta_{c,2}$. In the case of the bulk medium, we replace $\tilde{\rho}_x$ and $\tilde{C}_x$ in Eqs. (14) and (15) with their bulk counterparts, $\tilde{\rho}$ and $\tilde{C}$, respectively.

IV. RESULTS

Figures 3 and 4 present the normalized dynamic density, $\tilde{\rho}_x$, and complex compressibility, $\tilde{C}_x$, predicted using the
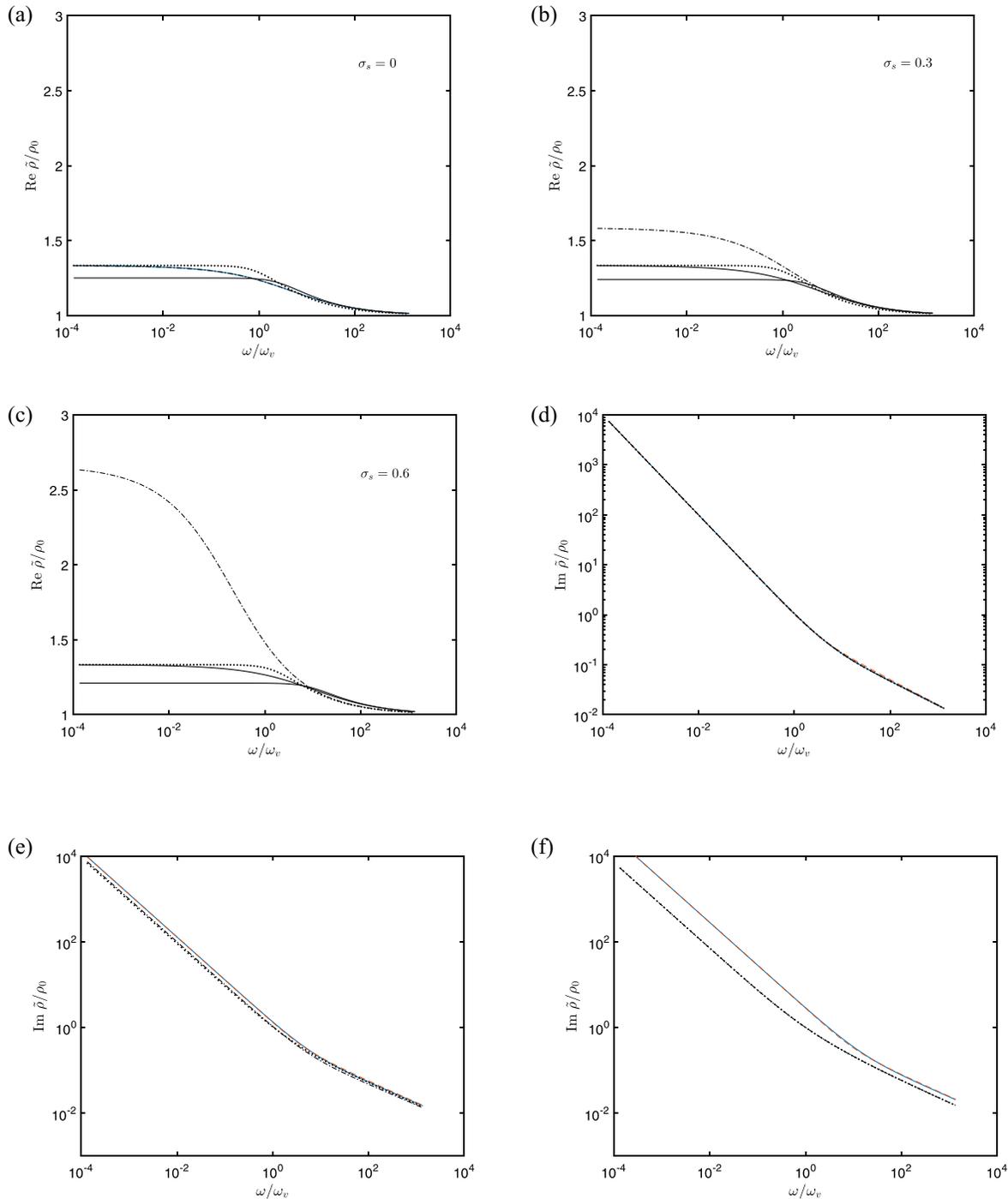
FIG. 3. (Color online) The normalized dynamic density of the fluid in a circular pore with a diameter of 1 mm. $\phi = 1$, $\alpha_\infty = 1$. Solid line: Padé approximation for the non-uniform pore; dash-dotted line: Padé approximation for the uniform pore; dashed line: Johnson *et al.* model; dotted line: Pride *et al.* model.

Horoshenkov *et al.*
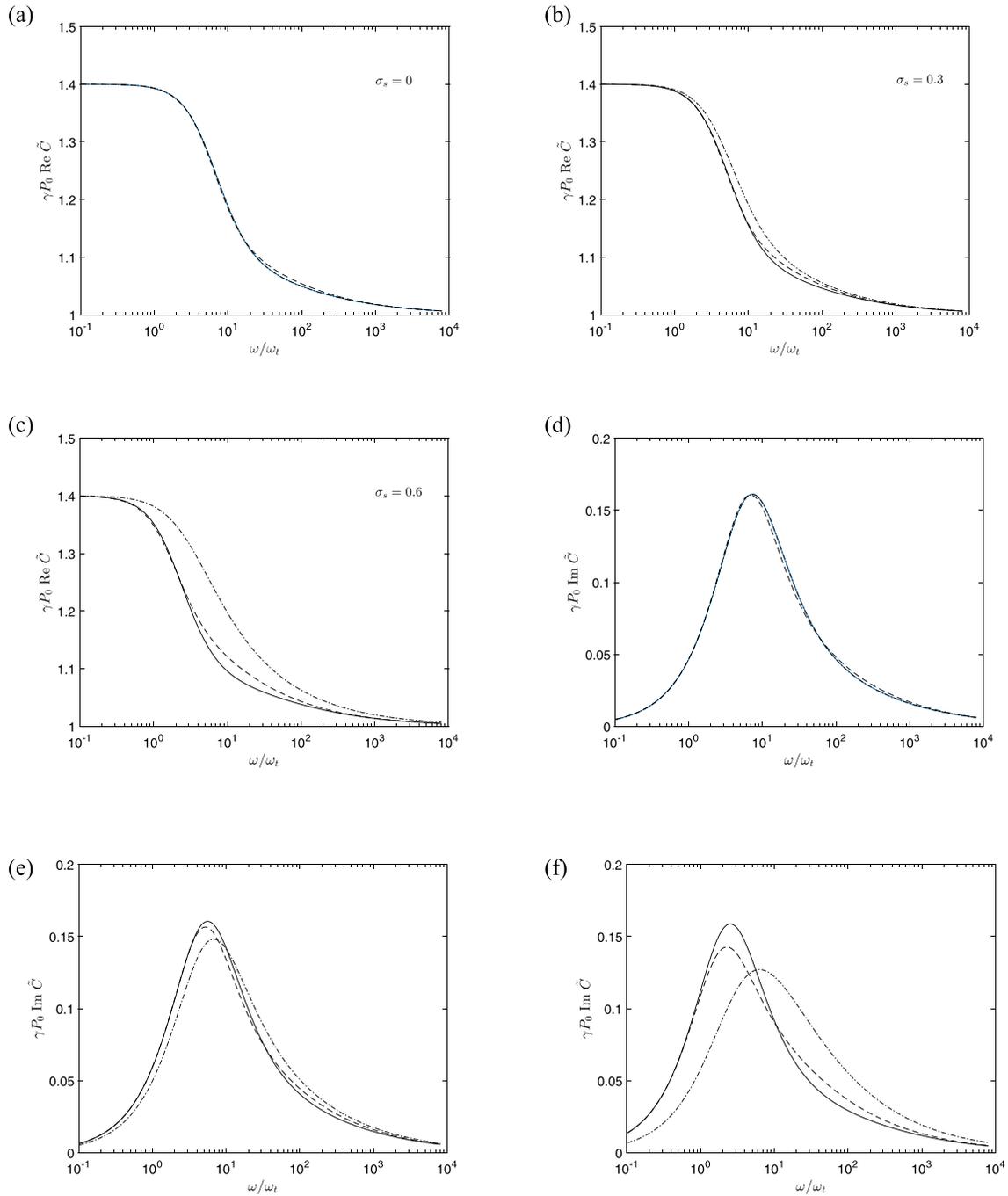
FIG. 4. (Color online) The normalized complex compressibility of the fluid in a circular pore with the diameter of 1 mm. $\phi = 1$, $\alpha_\infty = 1$. Solid line: Padé approximation for the non-uniform pore; dash-dotted line: Padé approximation for the uniform pore; dashed line: Champoux and Allard model.

Padé approximation model derived for the uniform circular cylindrical pore,[11] the JCA model,[2] the model of Pride *et al.*,[14] and the newly derived Padé approximations [Eqs. (64) and (68)] for a single non-uniform cylindrical pore case with $\sigma_s = 0$; 0.3; and 0.6. The dynamic density spectra are plotted against the dimensionless frequency scale, ω/ω_v, where $\omega_v = 8\eta/(\bar{s}^2 \rho_0)$ is the Biot characteristic frequency estimated for the median pore size $\bar{s}$. The complex compressibility spectra are also presented against the dimensionless frequency scale, ω/ω_t, where $\omega_t = \lambda_0/(\bar{s}^2 \rho_0 C_p)$ is the thermal characteristic frequency and λ_0 and C_p are the thermal conductivity and heat capacity of the fluid, respectively. In these calculations we assumed that the pore is filled with

fluid with $P_0 = 102 \, \text{kPa}$, $\gamma = 1.4$, $\rho_0 = 1.25 \, \text{kg/m}^3$, $\eta = 1.81 \times 10^{-5} \, \text{Pa s}$, $\lambda_0 = 0.0245 \, \text{W/m K}$, $C_p = 1003.5 \, \text{J/(kg K)}$ and that the diameter of this pore is $2\bar{s} = 1 \, \text{mm}$. We expressed the viscous and thermal characteristic lengths via $\bar{s}$ and σ_s using Eqs. (60) and (61). The flow resistivities were predicted with Eqs. (56) and (58).

The results presented in Fig. 3 for the dynamic density show that in the case when there is no pore size distribution in the medium ($\sigma_s = 0$) the imaginary part spectra predicted with each of the three models are very similar. The relative difference between the imaginary part spectra predicted with the JCA model[2] and the new Padé approximation model is within 8.5% for all values of σ_s considered in this work. The

Padé approximation for the uniform pore[11] and the new Padé approximation model are identical when $\sigma_s = 0$. The imaginary part spectra predicted with these two Padé approximation approaches begin to deviate significantly when $\sigma_s \neq 0$. The behavior of the imaginary part predicted with the original Padé approximation and the model of Pride *et al.* are almost identical. There is a noticeable difference between the real part predicted with the model of Johnson *et al.*, with the Padé approximation, and with the model of Pride *et al.* as the low-frequency limit is approached. The real part spectra predicted with the model of Johnson *et al.* asymptotically approaches the 5/4 limit, as suggested by the behavior of the real part in Eq. (22) and this limit does not depend on σ_s and is accounted for in the model of Pride *et al.*[14] The real part spectra predicted with the new Padé approximation asymptotically approaches the 4/3 limit as suggested by the behavior of the real part in Eq. (52), and this limit also does not depend on σ_s. The low-frequency asymptotic limit of the dynamic density predicted by the Padé approximation proposed in Ref. 11 depends on the value of σ_s as suggested by the behavior of the real part in Eq. (19). This dependence is exponential, so that the low-frequency limit of the real part of the density predicted by this model is higher than those predicted by the Johnson *et al.* model and by the Padé approximation for the uniform pore[11] (see Fig. 3).

The results for the complex compressibility spectra presented in Fig. 4 suggest that the three models agree very well in the case when $\sigma_s = 0$. The predictions by the two Padé approximations are identical. The relative difference between the imaginary part spectra predicted with the Champoux-Allard model[2] and the new Padé approximation model is within 7% for $\sigma_s = 0$. The relative difference between the real part of the spectra predicted with the Champoux-Allard model[2] and the new Padé approximation model is within 6% for $\sigma_s = 0$. This difference is not noticeably affected by the value of σ_s. Similarly, the relative difference between the imaginary part of spectra predicted with the Champoux-Allard model[2] and the new Padé approximation model does not noticeably change with the change of σ_s. However, there is a very large relative difference between the dynamic density spectra predicted with the Champoux-Allard model and with the original Padé approximation proposed for the uniform pores. In the case of $\sigma_s = 0.3$, the maximum difference is approximately 25%. In the case of $\sigma_s = 0.6$, this difference is approximately 90%.

V. CONCLUSIONS

The results presented in this paper show that there is a clear interdependence between the parameters of the pore size distribution and characteristic viscous (Λ) and thermal (Λ') lengths. In the particular case, when the pore size distribution can be assumed log-normal, it has been shown that for a material with uniform circular cylindrical pores the viscous characteristic length[1] and the standard deviation in the log-normal pore size (σ_s) (Ref. 11) this relation is $\Lambda = \bar{s}e^{-1/2(\sigma_s \ln 2)^2}$. It has also been shown that the asymptotic behavior of the real part of the dynamic density derived for $\omega \to 0$ in the case of pore size distribution approach[11] and

the approach of Pride *et al.*[14] can be matched exactly if the Pride parameter is set to $\beta = 4/3 e^{4(\sigma_s \ln 2)^2} - 1$.

In the case of porous media with non-uniform circular cylindrical pores it has been shown that the relation between the viscous characteristic length and the standard deviation in the log-normal pore size is $\Lambda = \bar{s}e^{-5/2(\sigma_s \ln 2)^2}$. The relation between the thermal characteristic length and the standard deviation in the log-normal pore size is $\Lambda' = \bar{s}e^{3/2(\sigma_s \ln 2)^2}$. This means that the ratio of the thermal to viscous characteristic lengths is controlled by the standard deviation in the pore size. If the pore cross-section is uniform, the ratio is $\Lambda'/\Lambda = 1$. If $\sigma_s \neq 0$, then this ratio becomes $\Lambda'/\Lambda = e^{4(\sigma_s \log 2)^2}$. For porous media with non-uniform pores, the relation between the viscous permeability[1] and the standard deviation in the log-normal pore size is $\kappa_0 = (\bar{s}^2/8)e^{-6(\sigma_s \log 2)^2}$. The relation between the thermal permeability[2] and the standard deviation in the log-normal pore size for this type of media is $\kappa'_0 = (\bar{s}^2/8)e^{6(\sigma_s \log 2)^2}$. In the case of a uniform pore ($\sigma_s = 0$), $\kappa_0 = \kappa'_0$, otherwise $\kappa'_0/\kappa_0 = e^{12(\sigma_s \ln 2)^2}$. The viscous characteristic length, thermal characteristic length and thermal permeability are notoriously difficult to measure non-acoustically. Therefore, these findings are particularly useful, because the median pore size and standard deviation in the pore size are routinely measurable parameters and the pore size distribution in a majority of porous media can be approximated with log-normal fit.

The asymptotic limits for the dynamic density and complex compressibility of the fluid in a medium with non-uniform pores have been used to derive new Padé approximations for these two quantities which enable us to calculate the acoustic characteristic impedance and wavenumber in this type of medium. The form of these approximations is very similar to that suggested in Ref. 11 for the case of a medium with uniform pores. The coefficients in these approximations are real and positive, which suggest that the Padé approximation model should satisfy the reality and causality conditions[18] which is important for time-domain modeling of sound propagation in porous media.

These finding suggest that the JCA model[1,2] and the model of Probe *et al.*[14] can be used with five directly measurable parameters, namely, flow resistivity (σ), porosity (ϕ), tortuosity (α_∞), median pore size ($\bar{s}$), and standard deviation in the pore size (σ_s). The viscous and thermal characteristic lengths can then be deduced from these parameters. As an alternative to the extensively validated JCA model, two newly derived Padé approximations [Eqs. (64) and (68)] can be used to predict the dynamic density and complex compressibility of the effective fluid in the non-uniform material pores using the same five intrinsic material parameters which are easily measurable non-acoustically. A comparison of the spectra for the real and imaginary parts of the dynamic density and complex compressibility predicted with the three models suggests that the predictions with the JCA model agree within 8.5% with those obtained with the new Padé approximation model [Eqs. (64) and (68)] for media with non-uniform pore. There can be large differences between the predictions made with the Padé approximation which was developed for media with uniform pores and that which we propose for media with non-uniform pores.

APPENDIX: THE BEHAVIOR OF THE INTEGRALS IN EQS. (39) AND (45)

Here we determine the low- and high-frequency limits for the two integrals which we derived in Sec. III. We express the integrals in the numerators in equations (39) and (45) in terms of σ_s, $\bar{\varphi}$, and φ,

$$I_\rho = \int_{-\infty}^{+\infty} \rho_x(\omega, \varphi) 2^{2\varphi} e^{-(\varphi - \bar{\varphi})^2/2\sigma_s^2} d\varphi \qquad (A1)$$

and

$$I_C = \int_{-\infty}^{+\infty} C_x(\omega, \varphi) 2^{-2\varphi} e^{-(\varphi - \bar{\varphi})^2/2\sigma_s^2} d\varphi. \qquad (A2)$$

It is easy to show that the integrals in the denominators of Eqs. (39) and (45) expressed in terms of σ_s, $\bar{\varphi}$, and φ simply reduce to

$$I_{1/A} = \int_{-\infty}^{+\infty} 2^{2\varphi} e^{-(\varphi - \bar{\varphi})^2/2\sigma_s^2} d\varphi = \sqrt{2\pi} \sigma_s 2^{2\bar{\varphi}} e^{2\sigma_s^2 \log^2 2} \qquad (A3)$$

and

$$I_A = \int_{-\infty}^{+\infty} 2^{-2\varphi} e^{-(\varphi - \bar{\varphi})^2/2\sigma_s^2} d\varphi = \sqrt{2\pi} \sigma_s 2^{-2\bar{\varphi}} e^{2\sigma_s^2 \log^2 2}. \qquad (A4)$$

Integral (A1) is effectively

$$I_{\rho, \omega \to 0} = \rho_0 \left(4/3 I_{1/A} - \frac{8\eta}{i\omega\rho_0} \int_{-\infty}^{+\infty} 2^{4\varphi} e^{-(\varphi - \bar{\varphi})^2/2\sigma_s^2} d\varphi \right) + O(\omega^4), \qquad (A5)$$

which reduces to ($\bar{s} = 2^{\bar{\varphi}}$)

$$I_{\rho, \omega \to 0} = \rho_0 I_{1/A} \left(4/3 - \frac{8\eta e^{6\sigma_s^2 \log^2 2}}{i\omega\rho_0 \bar{s}^2} \right) + O(\omega^4). \qquad (A6)$$

Similarly, integral (A2) for the low-frequency limit of the complex compressibility is

$$I_{C, \omega \to 0} = \frac{1}{\gamma P_0} \left(\gamma I_A - \frac{i\omega\rho_0 N_{Pr}(\gamma - 1)}{8\eta} \right. \\ \left. \times \int_{-\infty}^{+\infty} 2^{-4\varphi} e^{-(\varphi - \bar{\varphi})^2/2\sigma_s^2} d\varphi \right) + O(\omega^4), \qquad (A7)$$

which reduces to

$$I_{C, \omega \to 0} = \frac{I_A}{\gamma P_0} \left(\gamma - (\gamma - 1) \frac{i\omega\rho_0 N_{Pr} \bar{s}^2 e^{6\sigma_s^2 \log^2 2}}{8\eta} \right) + O(\omega^4). \qquad (A8)$$

The remaining high-frequency limit integrals for the above quantities are

$$I_{\rho, \omega \to \infty} = \rho_0 \left(I_{1/A} + 2\sqrt{\frac{\eta}{i\omega\rho_0}} \int_{-\infty}^{+\infty} 2^{3\varphi} e^{-(\varphi - \bar{\varphi})^2/2\sigma_s^2} d\varphi \right) + O(\omega^{-1}), \qquad (A9)$$

which reduces to

$$I_{\rho, \omega \to \infty} = \rho_0 I_{1/A} \left(1 + \frac{2}{\bar{s}} \sqrt{\frac{\eta}{i\omega\rho_0}} e^{5/2\sigma_s^2 \log^2 2} \right) + O(\omega^{-1}) \qquad (A10)$$

and

$$I_{C, \omega \to \infty} = \frac{1}{\gamma P_0} \left(I_A - 2\sqrt{\frac{\eta(\gamma - 1)}{i\omega\rho_0 N_{Pr}}} \right. \\ \left. \times \int_{-\infty}^{+\infty} 2^{-\varphi} e^{-(\varphi - \bar{\varphi})^2/2\sigma_s^2} d\varphi \right) + O(\omega^{-1}), \qquad (A11)$$

which reduces to

$$I_{C, \omega \to \infty} = \rho_0 I_A \left(1 - \frac{2(\gamma - 1)}{\bar{s}} \sqrt{\frac{\eta}{i\omega\rho_0 N_{Pr}}} e^{-3/2\sigma_s^2 \log^2 2} \right) + O(\omega^{-1}). \qquad (A12)$$

[1] D. L. Johnson, J. Koplik, and R. Dashn, "Theory of dynamic permeability and tortuosity in fluid-saturated porous media," J. Fluid Mech. 176, 379–402 (1987).

[2] Y. Champoux and J. F. Allard, "Dynamic tortuosity and bulk modulus in air-saturated porous media," J. Appl. Phys. 70(4), 1975–1979 (1991).

[3] J.-F. Allard and N. Attala, Propagation of Sound in Porous Media: Modelling Sound Absorbing Materials (Wiley, Chichester, UK, 2009).

[4] J.-F. Allard and Y. Champoux, "New empirical equations for sound propagation in rigid frame fibrous materials," J. Acoust. Soc. Am. 91(6), 3346–3353 (1992).

[5] P. Leclaire, L. Kelders, W. Lauriks, C. Glorieux, and J. Thoen, "Determination of the viscous characteristic length in air-filled porous materials by ultrasonic attenuation measurements," J. Acoust. Soc. Am. 99(4), 1944–1948 (1996).

[6] J.-P. Groby, E. Ogam, L. De Ryck, N. Sebaa, and W. Lauriks, "Analytical method for the ultrasonic characterization of homogeneous rigid porous materials from transmitted and reflected coefficients," J. Acoust. Soc. Am. 127(2), 764–772 (2010).

[7] R. Panneton and X. Olny, "Acoustical determination of the parameters governing viscous dissipation in porous media," J. Acoust. Soc. Am. 119(4), 2027–2040 (2006).

[8] X. Olny and R. Panneton, "Acoustical determination of the parameters governing thermal dissipation in porous media," J. Acoust. Soc. Am. 123(2), 814–824 (2008).

[9] J. F. Allard, M. Henry, J. Tizianel, L. Kelders, and W. Lauriks, "Sound propagation in air-saturated random packings of beads," J. Acoust. Soc. Am. 104(4), 2004–2007 (1998).

[10] C. Perrot, F. Chevillotte, M. T. Hoang, G. Bonnet, F.-X. Bécot, L. Gautron, and A. Duval, "Microstructure, transport, and acoustic properties of open-cell foam samples: Experiments and three-dimensional numerical simulations," J. Appl. Phys. 111, 014911 (2012).

J. Acoust. Soc. Am. 139 (5), May 2016

Horoshenkov et al.   2473

[11]K. V. Horoshenkov, K. Attenborough, and S. N. Chandler-Wilde, "Padé approximants for the acoustical properties of rigid frame porous media with pore size distribution," J. Acoust. Soc. Am. **104**, 1198–1209 (1998).

[12]M. Abramovitz and I. A. Stegun, *Handbook of Mathematical Functions*, Sec. 9.6 of National Bureau of Standards, Applied Mathematics Series (Dover, New York, 1972).

[13]E. Limpert, W. A. Stahel, and M. Abbt, "Long-normal distributions across the sciences: Keys and clues," BioSci. **51**(5), 341–352 (2001).

[14]S. R. Pride, F. D. Morgan, and A. F. Gangi, "Drag forces in porous medium acoustics," J. Phys. Rev. B **47**, 4964–4978 (1993).

[15]Y. Champoux and M. R. Stinson, "On acoustical models for sound propagation in porous materials and the influence of shape factors," J. Acoust. Soc. Am. **92**(2), 1120–1131 (1992).

[16]M. R. Stinson and Y. Champoux, "Propagation of sound and the assignment of shape factors in model porous materials having simple pore geometries," J. Acoust. Soc. Am. **91**(2), 685–695 (1992).

[17]C. Perrot, F. Chevillotte, and R. Panneton, "Dynamic viscous permeability of an open cell aluminium foam: Computations versus experiments," J. Appl. Phys. **103**, 024909 (2008).

[18]K. V. Horoshenkov, "Control of road traffic noise in city streets," Ph.D. thesis, University of Bradford, Bradford, UK (1996), Chap. 2.